# Pool Boiling CHF Enhancement in an External Reactor Vessel Cooling (ERVC) Using Graphene Oxide

Min ho Lee [a], Hyo Heo [a], In Cheol Bang[a*]
[a]*School of Mechanical and Nuclear Engineering*
*Ulsan National Institute of Science and Technology (UNIST)*
*50 UNIST-gil, Ulju-gun, Ulsan, 44919, Republic of Korea*
[*]*Corresponding author: icbang@unist.ac.kr*

## 1. Introduction

A reactor pressure vessel (RPV) contains radioactive coolants and other irradiated in-core structures such as fuel assemblies. In accident condition, insufficient removal of decay heat makes in core structure melt and the RPV is heated. Although fuel melted, radioactive materials are mainly retained in the RPV as long as integrity of the RPV is maintained. In vessel retention through external reactor vessel cooling (IVR-ERVC) concept used to maintain RPV without melt through. However, this cooling capacity of decay heat is limited by critical heat flux (CHF) phenomena. After CHF, heat transfer coefficient drop drastically and according to Newton's cooling law, temperature difference needed to remove decay heat also sharply increases. Increase of the RPV surface temperature threatens the integrity of RPV and finally, the concept of IVR-ERVC is failed. To prevent CHF and keep the concept of IVR-ERVC, CHF enhancement on the outer surface of reactor pressure vessel is required. In the present study, graphene oxide (GO) coating was selected as method for enhancement of CHF. According to Seo et al., [1] porous graphene oxide coating is the most efficient for CHF enhancement in pool boiling about 91% enhanced maximum heat flux compared to bare surface. However, if geometry of heating surface is like RPV, CHF enhancement is not as efficient as case on the horizontal cases (J. Yang et al. [2]). Similarly Park et al. [3] did flow boiling experiments on ERVC geometry with graphene oxide nanofluid to enhancement CHF. Compared to distilled water, CHF was enhanced about 20%, also relatively smaller. Dizon et al. [4] showed that CHF enhancement ratio was different from the angular location of the lower head of reactor pressure vessel. They also suggested spray coating and this coating method was also proven by Kumar et al., [5]

## 2. Experimental method

### *2.1 Preparation of heating surface*

Boiling phenomena including CHF are considerably affected by the surface condition. Fouling is precipitation of materials on a solid surface which affects to the boiling phenomena. According to Guzzetta [6], in subcooled boiling regime, fouling acts as a kind of thermal insulator and degrade boiling heat transfer. Otherwise in nucleate boiling regime, depending on the structure of fouling, the fouling can enhance boiling heat transfer. To exclude fouling effect in the results, sand paper was used to polish up the heater surface.

### *2.2 Experimental apparatus*

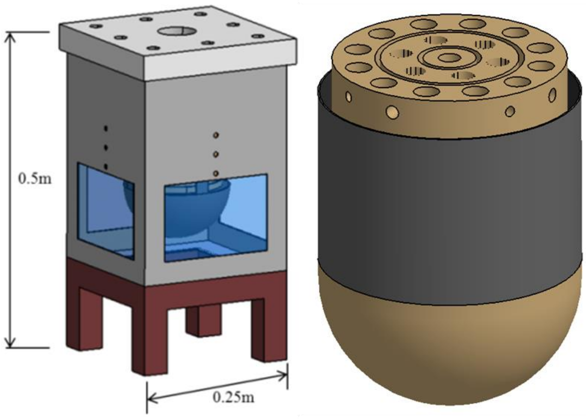


Fig. 1. Schematic of IVR-ERVC experimental apparatus

Figure 1 is overall shape of the experimental apparatus. The equipment is divided into three parts as boiling pool, heater and upper instruments. Boiling pool consisted of stainless steel structure and transparent glass window for visualization. Visualization was conducted through side faces and the window on the bottom face is for well-lighting. Heater is made of copper and cartridge heaters and thermocouples are sheathed in the heater. Radius of heater is about 74 mm, which is about 35 times scale down from reactor pressure vessel of APR 1400. Upper instruments are upper deck and condenser. Upper deck supports the cooper heater and penetrated by power cable and thermocouple line going out from heater to outside through upper deck. Reflux coil condensers were used to condense vapor of working fluid, and final heat sink is tap water flowing inside the coil of the condensers. Working fluid was selected as R-123 due to lower boiling point and latent heat compared to water. So we could get CHF relatively lower power and lower temperature than water, which is original working fluid of IVR-ERVC.

*2.3 Surface coating*

Porous structure of coating makes CHF enhancement. Porous structure is mainly generated during boiling procedure with the nanofluid. However, coating by boiling using small cap surrounding the heater was failed due to evaporation of nanofluid. Bigger cap or bigger coating pool can mitigate this problem but cannot solve the problem clearly. Therefore, in this study, spray coating method was used. Onto well heated surface, GO nanofluid was sprayed. When GO nanofluid contacts with well heated surface, the GO nanoparticles precipitated on the surface building porous structure. GO nanofluid was evenly sprayed on bare surface just after sand-papering. The surface temperature of well-heated surface was set as 150 ℃. Because boiling point of water in atmospheric pressure is 100 ℃ and superheat 50 ℃ for immediate evaporation of water.

*2.4 Test Matrix*

Many previous studies about coating with nanofluid quantify concentration of nanofluid as volume percent. Thus, volume percent was used to quantify concentration of nanofluid in this study. To observe clear distinction of appearance and enhancement compared to the bare surface, amount of nanofluid was fixed as 300ml but volume percent of nanofluid was varied as 0.01%, 0.03% and 0.05%. Each condition tested three times. Used amount of nanoparticle and amount of nanoparticle in unit area on the coated surface were listed in Table I.

Table I: Test matrix

| Used nanoparticle | GO | | |
|---|---|---|---|
| Volume percent of nanoparticle [%] | 0.01 | 0.03 | 0.05 |
| Volume of nanofluid [ml] | 300 | | |
| Mass of nanoparticle [mg] | 54 | 162 | 270 |
| Surface area [$cm^2$] | 494.9 | | |
| Coated mass in unit area [$mg/cm^2$] | 0.109 | 0.327 | 0.546 |

**3. Result and discussion**

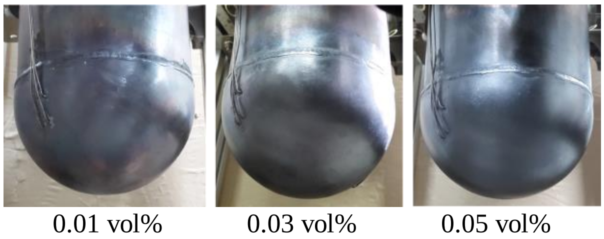

Fig. 2. GO coated surface

Figure 2 shows coated surfaces with GO nanofluid. The color of coated surface deepens as volume fraction of nanoparticle increases. In 0.05% case, the coated surface looks like silver-colored metal.

Table II: CHF value with GO concentration

| Unit [W] | Bare | 0.01% | 0.03% | 0.05% |
|---|---|---|---|---|
| Exp. 1 | 915.7 | 1110.3 | 1173.5 | 1238.4 |
| Exp. 2 | 895.2 | 1104.6 | 1167.7 | 1256.4 |
| Exp. 3 | 915.7 | 1131.9 | 1191.0 | 1274.6 |
| Average | 908.9 | 1115.6 | 1177.4 | 1256.5 |
| Enhancement ratio | - | 22.7% | 29.5% | 38.2% |

Table 2 shows experimental result of the CHF value. Maximum deviation of data from average of each condition was about 1.5 % in the second experiment in bare case. Under bare condition, the average power at CHF point was 908.9 W. However, in 0.01% volume percent case, CHF was occurred at 1115.6 W in average. It was 22.7% increased value compared to average power at CHF point in bare condition. In 0.03% volume percent case, average power at CHF was 1177.4 W and it is 29.5 % increase value. Similarly, in 0.05% volume percent case, average power at CHF was 1256.5W and it is 38.2% increase value.

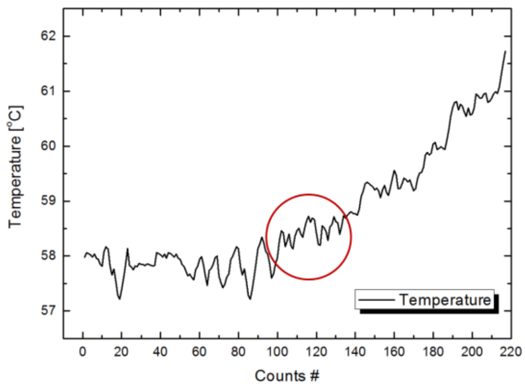

Fig. 3. Criteria for CHF determination

Actually, in this experiment, thermal mass and thermal inertia of copper heater was larger than other experiments, such as wire boiling or thin surface with thin heater boiling. CHF determination was based on thermocouple at the outmost and connection part between cylinder and hemisphere. Outmost thermocouple is most sensitive to temperature change of the boiling surface. And end of hemisphere has the highest heat flux in the experiments.

Visualization results showed difference before CHF and after CHF. After CHF, more vigorous boiling and expansion of bubble layer thickness along rising direction occurred. The bubble layer thickness at the connection part between cylinder and hemisphere, which was the region having the highest heat flux is the key difference between before CHF and after CHF. After CHF, unlikely before CHF, the bubble layer thickness was thicker than before CHF. This bubble layer disrupted the liquid supply into heating surface in CHF condition. As shown in Fig. 4, the behavior of vapor bubble was different before CHF and after CHF. The left column of this figure is bubble behavior just before CHF, 1000W. From the top, time step between each picture was 0.02 seconds. There was bubble wave formation from the bottom of hemisphere in the Fig. 4 (a). The bubbles rose along the hemisphere in the Fig. 4 (b). Finally, the bubble collapsed at the end of hemisphere in the Fig. 4 (c). The right column of the Fig. 4 is result at CHF case. These pictures show similar bubble wave behavior with that of CHF, bubble wave formation in the Fig. 4 (a), bubble layer rising in the Fig. 4 (b), and bubble layer collapse and another bubble wave formation from the bottom in the Fig. 4 (c).

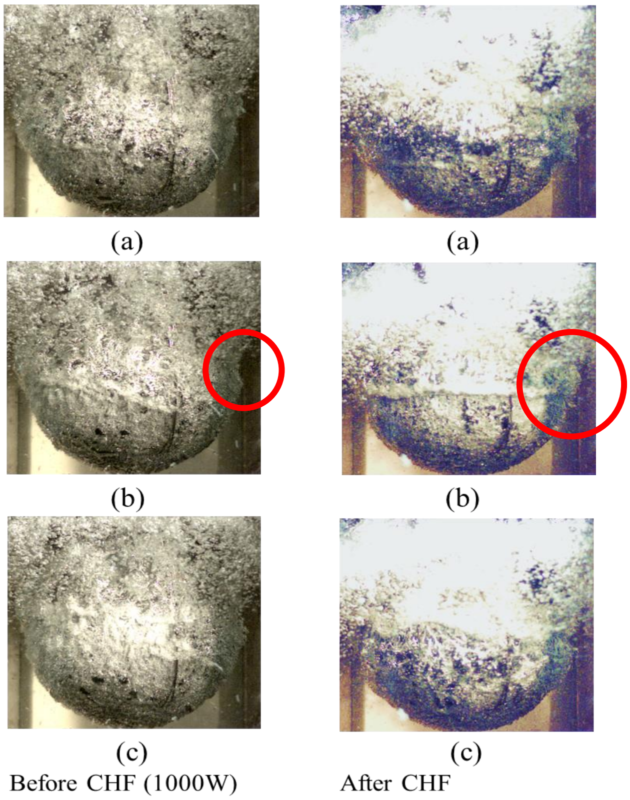


Fig. 4. Visualization of 0.01 vol% case before and after CHF

During procedure from the Fig. 4 (a) to (c), the bubble formation frequency was faster and the thickness of bubble wave layer was thicker and larger at CHF in red circle at both Fig. 4 (b). This was due to the increase of evaporation with increase of heat flux. The formation of bubble wave and its rising was at almost simultaneously in circumferential direction at CHF. Otherwise, before CHF, bubbles did not rise at once in circumferential direction. Overall bubble layer thickness was thicker at CHF case especially at the end of hemisphere.

## 4. Conclusion

To enhance CHF in IVR-ERVC concept, GO coating was used. Total power values at CHF were enhanced comparing to that of bare condition.

Visualization results showed more vigorous bubble behavior at CHF than before CHF. More amounts of bubbles are generated at each time and reproduction frequency was shorter than those of before CHF.

## ACKNOWLEDGEMENTS

This work was supported by the Nuclear R&D program (NRF-2013M2B2B1075734, NRF-2014M2A8A4021514) through the National Research Foundation of Korea (NRF) funded by the Korea government (MSIP).

## REFERENCES

[1] H. Seo, J. H. Chu, S. Y. Kwon and I. C. Bang, Pool boiling CHF of reduced graphene oxide, graphene, and SiC-coated surfaces under highly wettable FC-72, International Journal of Heat and Mass Transfer, vol.82, pp.490-502 2015.
[2] J. Yang, F. B. Cheung, J. L. Rempe, K. Y. Suh and S. B. Kim, Critical heat flux for downward-facing boiling on a coated hemispherical vessel surrounded by an insulation structure, Nuclear Engineering and Technology, vol.38, pp.139-146, 2006.
[3] S. D. Park and I. C. Bang, Flow boiling CHF enhancement in an external reactor vessel cooling channel using graphene oxide nanofluid, Nuclear Engineering and Design, vol.265, pp.310-318, 2013.
[4] M. B. Dizon, J. Yang, F. B. Cheung, J. L. Rempe, K. Y. Suh and S. B. Kim, Effects of Surface Coating on the Critical Heat Flux for Pool Boiling from a Downward Facing Surface. Journal of Enhanced Heat Transfer, vol.11, pp.133-150, 2004.
[5] S. Kumar, S. Suresh, Q. Yang, C.R. Aneesh, An experimental investigation on flow boiling heat transfer enhancement using spray pyrolysed alumina porous coatings, Applied Thermal Engineering, vol.71, pp.508-518, 2014.
[6] A. Guzzetta, Modeling the effects of fuel rod CRUD formation on boiling heat transfer in a pressurized water reactor using Eulerian two-fluid CFD, Master Dissertation, The Pennsylvania State University, Pennsylvania USA, 2010.